**Summary:** Reaction calorimetry is an efficient tool used to obtain kinetic, thermodynamic and safety data. A reaction calorimeter, RC1*e-HP350*, developed in collaboration with Mettler-Toledo GmbH, allows investigating chemical reactions under supercritical conditions. The main technical difference, compared with a classical liquid system, is that the whole reactor volume is occupied by the media. Heat transfer analysis in supercritical carbon dioxide ($scCO_2$) by the Wilson plot method shows that the behavior of the internal heat transfer coefficient in $scCO_2$ is the opposite of the one observed for classical liquid. In $scCO_2$ the lower the temperature (above the critical point) the better the internal heat transfer coefficient. The evolution of $scCO_2$ thermodynamical and transport properties near the critical point are responsible for this behavior. The dispersion polymerization of methyl methacrylate in $scCO_2$, with the polydimethylsiloxane monomethacrylate as stabilizer, is used as a model reaction. A polymerization reaction enthalpy of $-56.9 \pm 2.2\ kJ \cdot mol^{-1}$ is determined, being in good agreement with previously reported data. The results presented illustrate the accuracy of the heat balance model used and emphasize the potential of reaction calorimetry for the promotion of supercritical fluids technologies.

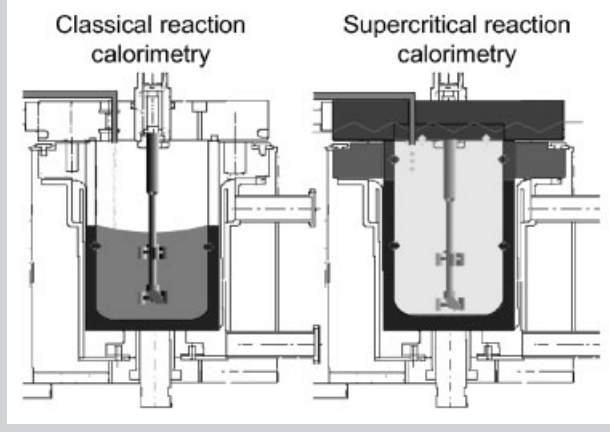


Technical comparison between liquid and supercritical reaction calorimetry.

# Reaction Calorimetry in Supercritical Carbon Dioxide - Methodology Development -

*Sophie Fortini, Frédéric Lavanchy, Thierry Meyer**

Institute of Chemical Sciences and Engineering, Swiss Federal Institute of Technology, 1015 Lausanne, Switzerland
Fax: +41 21 693 3190; E-mail: thierry.meyer@epfl.ch

Received: March 26, 2004; Revised: May 14, 2004; Accepted: June 14, 2004; DOI: 10.1002/mame.200400077

**Keywords:** carbon dioxide; dispersion; heat transfer; polymerization; reaction calorimetry; supercritical fluid

## Introduction

Supercritical fluids (SCFs) are of great technological interest because they exhibit properties which lie between those of conventional liquids and gases. Their physical properties reveal, at pressures and temperatures near the critical point, spectacular changes over a wide range. This allows the solvating power of a solvent in supercritical state to be effectively tuned by varying the pressure and/or the temperature. This characteristic has led to the development of supercritical fluid processes applied to extractions[1] and more recently to chemical reactions.[2] Most of the studies focus on supercritical carbon dioxide ($scCO_2$) being considered as a ''green''-solvent, accessible and inexpensive, non-toxic and non-flammable. In the near future, the growing interest in replacing harmful organic solvents and reducing aqueous waste will emphasize the development of supercritical fluid processes. For SCF applications a financial balance has to be drawn up in order to evaluate the process viability, taking into account that infrastructure and energy costs for gas compression may lead to strong limitations.

Reaction calorimetry is a common tool based on heat flows and heat balance measurements. It finds most of its applications in the determination of kinetics parameters, in the evaluation of data for process safety analysis and process optimization[3] as well as phase equilibrium and phase transition studies.[4] The reaction calorimeter is composed of a 1.3 L high pressure reactor coupled to a Mettler-Toledo RC1*e* thermostat. The set-up gives the opportunity to work

 DOI: 10.1002/mame.200400077 

at larger scale with reaction conditions close to those of industrial reactors. In fact, most of the studies related to SCF chemical reaction applications are realized in small-scale batch or tubular reactors (1–60 $cm^3$). Until now very few publications are dealing with calorimetry applied to the supercritical phase. The presented results describe, to our knowledge, the first development and use of a reaction calorimeter for supercritical field applications.[5]

It is important for the polymer industry to find alternatives process routes decreasing the impact of solvent emissions to the environment. This has motivated the development of polymerization reaction processes in $scCO_2$.[6,7] Many monomers exhibit good solubility in $scCO_2$.[8] However, it is a rather poor solvent for most high molecular weight polymers except for some fluoropolymers and silicones.[9–11] The latter are often used as sterical stabilizers in the dispersion polymerization of vinyl polymers such as poly(methyl methacrylate)[12–18] and poly(styrene).[19]

The dispersion polymerization of methyl methacrylate in $scCO_2$, using the commercially available polydimethylsiloxane monomethacrylate as stabilizer, is used as a model reaction.[20] These preliminary results will serve to validate the heat transfer model and also to illustrate the great potential of reaction calorimetry as a thermo-analytical tool.

## Supercritical Reaction Calorimeter

### *Reaction Calorimeter*

The reaction calorimeter for supercritical thermal analysis has been developed in collaboration with Mettler-Toledo GmbH. The reaction vessel (HP 350, Premex, Switzerland) is a 1.3 L high pressure autoclave operating up to 350 bar and 300 °C (Figure 1). The reactor, is coupled to a thermostat unit to control the reaction temperature, $T_r$. The reactor is equipped with a magnetic drive, a 25 W calibration heater, a Pt100 reactor temperature sensor and a pressure sensor. The calorimeter allows working in three different operating modes; *adiabatic*, *isoperibolic*, and *isothermal*.[21]

### *Supercritical Calorimetric Challenge*

Generally, in ''classical'' reaction calorimetry only the liquid phase is taken into account in the heat balance. This means that the gas phase in equilibrium is neglected due to its small contribution in terms of heat transfer and heat capacity. The situation complicates with supercritical fluids as soon as they occupy all the available volume. The whole inner reactor surface has to be perfectly controlled thermally when working with supercritical fluids. In our case, the cover and the flange temperature are adjusted on-line to $T_r$ in order to neglect the heat accumulation term (Figure 2).

### *Heat Balance Equation*

The most important assumptions in reaction calorimetry are: temperature and concentration homogeneity. Then, the energy balance for a semi-batch process is given by:

$$Q_r + Q_c + Q_{stir} = Q_{acc} + Q_{dos} + Q_{flow} + Q_{loss} \quad (1)$$

where $Q_r$ is the heat generation rate of the reaction, [W]. $Q_c$ is the heat delivered by the calibration probe, [W]. $Q_{stir}$ is the heat input by the stirrer, [W]. $Q_{acc}$ is the accumulation term, [W]. $Q_{dos}$ corresponds to the amount of heat due to addition of reactants, [W]. $Q_{flow}$ is the heat flow through the reactor wall, [W]. $Q_{loss}$ is the heat losses to the surroundings, [W].

The simplified heat balance equation used for the preliminary polymerization experiments is given by:[20]

$$Q_r = Q_{flow} \quad (2)$$

$$Q_{flow} = U \cdot A \cdot (T_r - T_j) \quad (3)$$

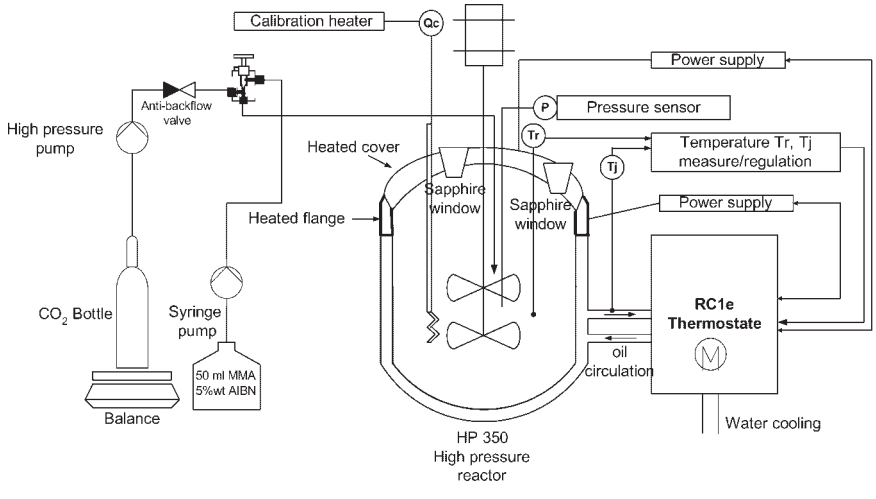


Figure 1. Technical scheme of the reaction calorimeter.

 

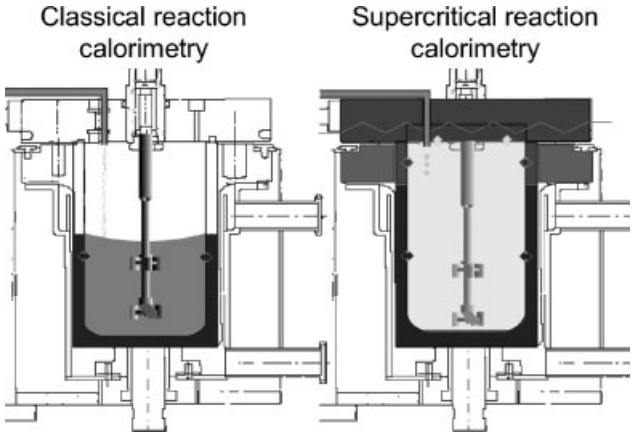


Figure 2. Technical comparison between liquid and supercritical reaction calorimetry.

$U$ is the overall heat transfer coefficient, $[W \cdot m^{-2} \cdot K^{-1}]$. $A$ is the heat exchange surface, $[m^2]$. $T_r$ is the temperature of the media, [K]. $T_j$ is the jacket temperature, [K].

The overall heat transfer coefficient, $UA$, could be measured online using a calibration probe delivering an amount of heat, $Q_c$, around 25 W and using Equation (4):

$$UA = \frac{\int_{t1}^{t2} (Q_c - Q_b) \cdot dt}{\int_{t1}^{t2} (T_r - T_j) \cdot dt} \quad (4)$$

where $Q_b$ is the baseline term, [W]. $t$ is the time, [s].

The terms $Q_{loss}$ and $Q_{stir}$ in Equation (1) can be taken as constant during an isothermal experiment and are introduced in the baseline, $Q_b$.[21] The measurement of $UA$ at the beginning and at the end of the reaction is sufficient for reactions with little variations of the physico-chemical properties. For polymerizations, the analysis may not be trivial due to the change of medium viscosity during the polymerization process. In this case, both terms $UA$ and $Q_{stir}$, which are directly related to the viscosity, may vary during the polymerization. In our case, the influence of $Q_{stir}$ was limited choosing a ''proportional to conversion'' baseline type. The baseline $Q_b$ takes into account all the effects on the heat generation rate $Q_r$ that are not directly measurable. The most important are heat flows which have been neglected in Equation (1) or changes in the calibration factors (e.g. $U$). The baseline should describe the signal profile which would be recorded if no reaction occurs. This is of particular importance if $Q_r$ is not the same at the start and the end of a heat generation peak. A mean value of $UA$ was used for the heat flow term. The accumulation term in Equation (1), $Q_{acc}$, can also be neglected as soon as the system is working in a perfect isothermal mode. The dosing term, $Q_{dos}$, can be neglected only when a small quantity is added or when $T_{dos}$ equals $T_r$.

For single reactions or one dominant reaction, such as the propagation reaction in free radical or chain polymerization processes, $Q_r$ is directly proportional to the measured heat flow and the reaction enthalpy is given by:

$$\Delta_r H = \frac{\int_{t0}^{tf} (Q_r - Q_b) \cdot dt}{m_{ro} \cdot X} \quad (5)$$

where $\Delta_r H$ is the polymerization enthalpy, $[J \cdot kg^{-1}]$. $m_{ro}$ is the initial amount of monomer, [kg]. $X$ is the monomer conversion when the polymerization is stopped ($t_f$).

### *Wilson Plot Analysis*

Wilson plot analysis allows measuring the overall heat transfer coefficient, $U$.[22] The inverse of the overall heat transfer coefficient, $1/U$, can be expressed as a sum of three heat transfer resistances:

$$\frac{1}{U} = \frac{1}{h_r} + \frac{e}{\lambda_w} + \frac{1}{h_{oil}} \quad (6)$$

where $h_r$ is the internal heat transfer coefficient, $[W \cdot m^{-2} \cdot K^{-1}]$. $e$ is the jacket wall thickness, [m]. $\lambda_w$ is the thermal conductivity of the metallic wall, $[W \cdot m^{-1} \cdot K^{-1}]$. $h_{oil}$ is the heat transfer coefficient through the coolant film, $[W \cdot m^{-2} \cdot K^{-1}]$.

In Equation (6), the last two terms are independent of the reaction medium and could be summed in $\varphi$, being the external heat transfer coefficient, $[W \cdot m^{-2} \cdot K^{-1}]$ leading to:

$$\frac{1}{U} = \frac{1}{h_r} + \frac{1}{\varphi} \quad (7)$$

The internal heat transfer coefficient can be expressed using the dimensionless correlation relating the Nusselt number (Nu) to the Reynolds (Re) and Prandtl numbers (Pr):

$$Nu = C \cdot Re^a \cdot Pr^b \cdot \left(\frac{\mu}{\mu_w}\right)^c = \frac{h_r \cdot d_r}{\lambda} = C \cdot \left(\frac{N \cdot d_s^2 \cdot \rho}{\mu}\right)^a \cdot \left(\frac{c_p \cdot \mu}{\lambda}\right)^b \cdot \left(\frac{\mu}{\mu_w}\right)^c \quad (8)$$

where $d_r$ is the reactor internal diameter, [m]. $\lambda$ is the bulk thermal conductivity, $[W \cdot m^{-1} \cdot K^{-1}]$. $\mu$ is the bulk dynamic viscosity, $[kg \cdot m^{-1} \cdot s^{-1}]$. $N$ is the stirrer rotation speed, $[s^{-1}]$. $d_s$ is the stirrer characteristic diameter, [m]. $\rho$ is the bulk density, $[kg \cdot m^{-3}]$. $c_p$ is the bulk constant pressure heat capacity, $[J \cdot kg^{-1} \cdot K^{-1}]$ and $C$ is a constant, [-].

The exponent $a$ for the Reynolds number in the Nusselt equation is usually 2/3 for a stirred tank reactor equipped with a turbine in liquid media.[23] Exponent $b$ for the Prandtl number is 1/3. The viscosity ratio, for which exponent $c$ is usually 0.14, can be neglected since the maximum temperature difference between the bulk and the wall is less than

1 °C in isothermal mode. The combination of Equation (7) and (8) allows expressing the inverse of the global heat transfer coefficient as a function of the turbine's rotation speed:

$$\frac{1}{U} = \frac{1}{C' \cdot N^{2/3}} + \frac{1}{\varphi} \quad (9)$$

## Experimental Part

Carbon dioxide (purity 99.9%, Carbagaz, Switzerland) is delivered using a bottle mounted on a balance (Mettler-Toledo GmbH, Switzerland) and connected to a $CO_2$ pump (NWA GmbH, Germany). The Wilson experiments procedure is as follows: The reactor is filled and purged two times with about 50 g of $CO_2$. Then the reactor is filled up to a given mass. Eight stirring speeds between 100 and 2500 rpm are tested at four isotherms: 32, 35, 50, 100 °C for different densities.

The MMA dispersion polymerization in $scCO_2$ using the PDMS macromonomer as stabilizer is realized using the following products: The stabilizer ($\overline{M}_w \approx 5\,000$ g · mol$^{-1}$) supplied by ABCR (Germany), the initiator (2,2′-azoisobutyronitrile, AIBN) supplied by Fluka, and the monomer (methyl methacrylate, MMA) supplied by BASF (Germany) are used without further purification. The reaction vessel is charged with monomer (200 g) and the required amount of stabilizer (25 g), then closed and filled with $CO_2$ (around 800 g). Then the temperature is raised to 80 °C. At this temperature, a 50 mL MMA solution containing 5.1 wt.-% AIBN is added into the reactor under pressure using a syringe pump (100 DX, ISCO Inc.). The final ratio of AIBN/MMA is 1 wt.-% for all the experiments. After 4 h, the reactor content is quenched by cooling and venting $CO_2$ through a discharge tube. The conversion of methyl methacrylate is evaluated gravimetrically. The polymer obtained is characterized in terms of molecular weight distribution (TDA 300, Viscotek), particle size distribution (Mastersizer 2000, Malvern Instruments), and morphology by electron microscopy (SEM). The polymer powder is dispersed in hexane for the measurement of particle size distribution.

## Results and Discussion

### *Heat Transfer*

The linearity of the Wilson plot and the validity of the Nusselt correlation is confirmed in Figure 3(a). The internal heat transfer coefficient, $h_r$, can be expressed as a function of the rotation speed at the 2/3 power. The linear trend indicates that the overall heat transfer coefficient, $U$, follows the Wilson plot regression for all the studied temperatures and stirring speeds except at 100 rpm. The deviation of the model at 100 rpm is explained by temperature and density inhomogeneities in the medium due to insufficient stirring.

It is well known that for pressures and temperatures close to the critical point, most of the physico-chemical properties exhibit variations over a wide range. The behavior of $h_r$ is inverse to the one observed for classical liquid systems.

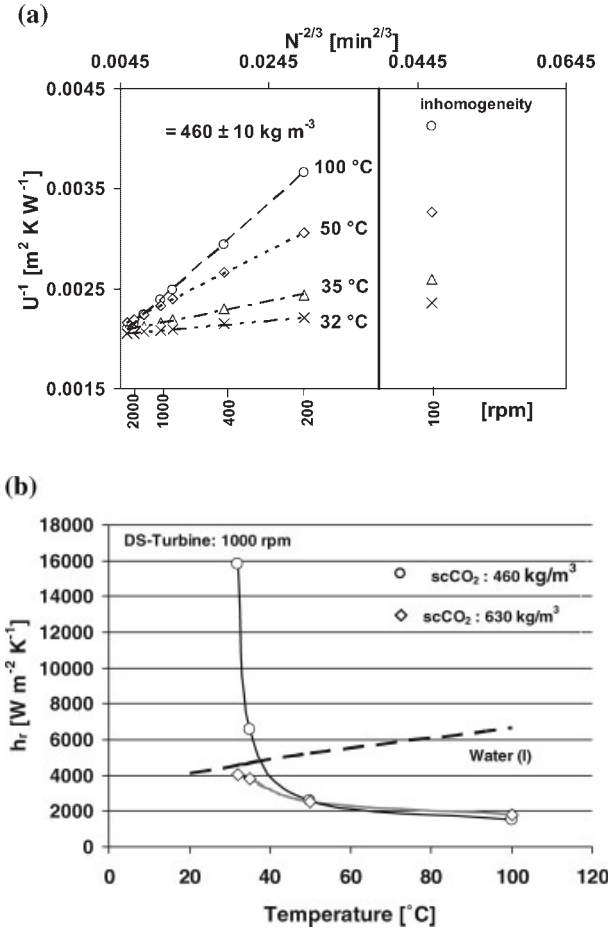


Figure 3. (a) Wilson plot for the double-stage turbine and $scCO_2$ density of 460 kg · m$^{-3}$. (b) Comparison of $h_r$ behavior for water and $scCO_2$ at a stirring speed of 1 000 rpm.

$h_r$ improves asymptotically close to the critical point of $scCO_2$. For liquid water this tendency is not observed and $h_r$ increases quite linearly with temperature (Figure 3(b)). The particular behavior of $h_r$ for $scCO_2$ is mainly due to the behavior of $c_p$, $\lambda$ near the critical point. As illustrated in Figure 4, the thermal conductivity can rise by two orders of magnitude close to critical point, the same behavior is observed for the heat capacity.[5] The combination of $\lambda$ and $c_p$ behavior explains the asymptotic divergence of the internal heat transfer coefficient in the vicinity of the critical point as the latter is proportional to $\lambda^{2/3}$ and $c_p^{1/3}$.

The intercept at infinite rotation speed in Figure 3(a) corresponds to the external heat transfer coefficient, $\varphi$. The intercept of the regressions performed at different temperatures indicates clearly an opposite effect of temperature on $h_r$ and $\varphi$. $\varphi$ improves with increasing temperature, mainly due to the decrease of the coolant viscosity with temperature.

### *Dispersion Polymerization of Methyl Methacrylate*

The results for the dispersion polymerization of methyl methacrylate in $scCO_2$ at 80 °C are summarized in Table 1.

 

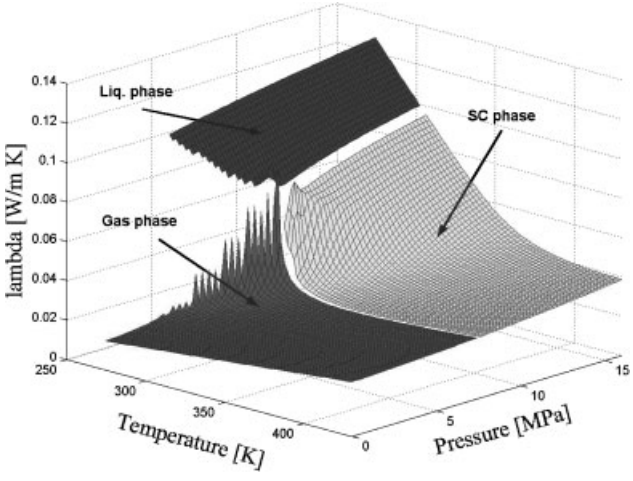


Figure 4. Three-dimensional view of a P-T-$\lambda$ phase diagram for $CO_2$.

The characteristic reaction time is 180 min. $P_0$ is the pressure measured before the addition of the initiator/MMA solution and $P_r$ the pressure at the end of the polymerization. It is observed in Figure 6 that the pressure first decreases to a minimum and then slightly increases reaching a value lower than the initial pressure. Several authors[14,24] show that the pressure can either increase or decrease with time during a batch dispersion polymerization in $scCO_2$. It appears that the pressure behavior depends on the initial pressure in the system. The actual data do not allow defining a precise upper limit from which a decrease in pressure is observed rather than an increase. This behavior change could be estimated between 230 and 300 bar. The pressure decrease can be understood by taking into account the change in molar volume of a vinyl monomer to the corresponding polymer. Lepiller and Beckman[24] attributed the anomalous pressure variation, with respect to the initial pressure in the reactor, to the non ideal behavior of the ternary system (monomer-$CO_2$-polymer).

Both polymerizations conducted with 10 wt.-% PDMS macromonomer respectively at stirring speed of 400 and 600 rpm yield a fine white powder with high molecular weight at monomer conversion higher than 90%. The well defined spherical morphology is observable by scanning electron microscopy (Figure 5(a)). The term $D$(v, 0.9) in Table 1 means that 90% of the particles have a diameter under the given value. Figure 5(b) gives an example of the narrow particle size distribution obtained for the polymerization at 400 rpm.

At commercial scale, stirring is essential to ensure temperature homogeneity and to avoid thermal runaway. However, it is well known that dispersion polymerizations in $scCO_2$ can be destabilized under efficient stirring speed due to additional termination mechanism by interaction with the reactor metallic wall[13] or due to shear forces. The relative stability under stirring depends on the characteristics of the stabilizer (molecular weight, backbone, morphology). Moreover, its relative proportion with respect to

Table 1. Experimental conditions and results of the dispersion polymerizations.

| rpm | $P_0$ | $P_r$ | Conversion | $\bar{M}_w$ | PDI | $d_p$ (SEM) | $D$(v, 0.9) |
|---|---|---|---|---|---|---|---|
| | bar | bar | % | kg · mol$^{-1}$ | | µm | µm |
| 400 | 270 | 304 | 94 | 117 | 1.9 | 0.5–2.1 | 1.8 |
| 600 | 257 | 296 | 92 | 108 | 2.6 | 0.5–2.0 | 1.8 |

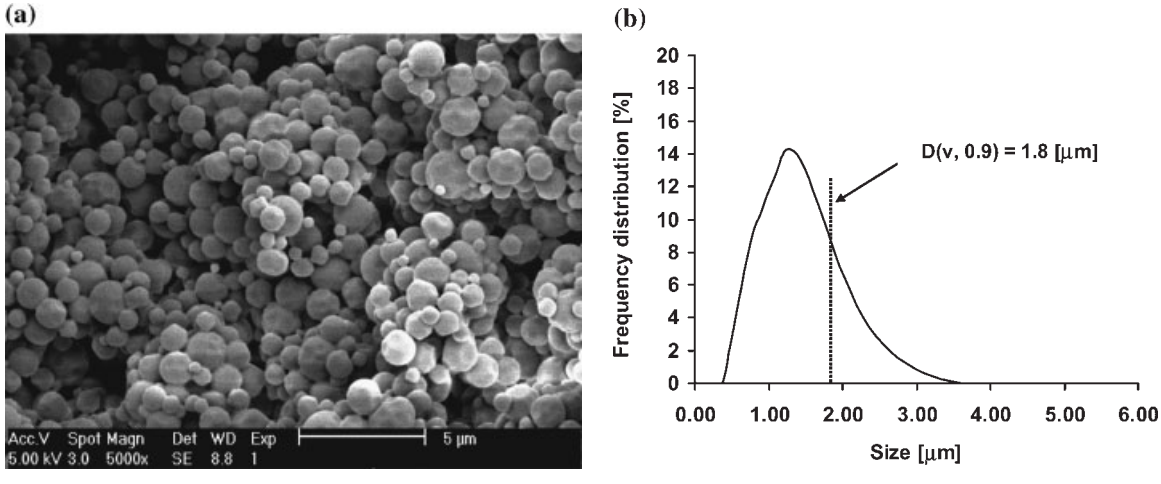


Figure 5. (a) SEM micrograph (5 000×) of PMMA produced at 400 rpm. (b) Particle size distribution of PMMA produced at 400 rpm.

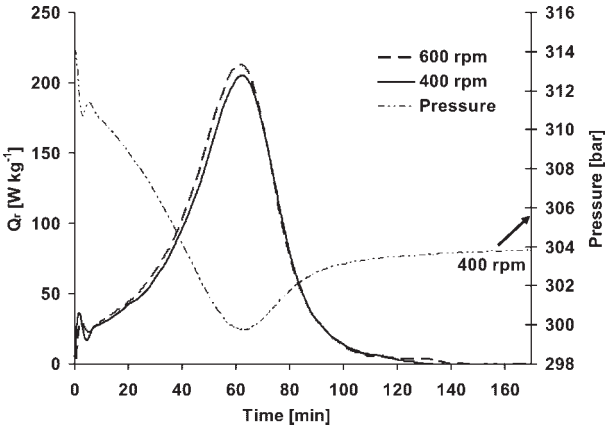


Figure 6. Evolution of the heat released by MMA polymerization at 400 and 600 rpm.

monomer is a key parameter for successful and effective dispersion polymerization at high stirring speed. It is observed in Figure 6 that the heat released, calculated with respect to the total weight of monomer, does not depend on stirring speed. Moreover, the good reproducibility of the reaction calorimeter is confirmed. By the integration of the thermal curves, the enthalpy of polymerization can be calculated as $-56.9 \pm 2.2$ kJ · mol$^{-1}$ and is in good agreement with the literature's value of $-57.8$ kJ · mol$^{-1}$ obtained in conventional solvent.[25] The error of 2.2 kJ · mol$^{-1}$ is a standard deviation calculated from a series of 7 measurements. This result reveals all the potential of reaction calorimetry for supercritical fluid investigations and polymerization monitoring. Wang et al. discussed in 2003, the monitoring of polymerizations in $scCO_2$ using a compensation calorimeter with a total volume of 60 mL.[26] They concluded that this technique was not of high precision mainly due to calorimetric problems. They obtained an enthalpy of polymerization from $-52.6$ to $-59.7$ kJ · mol$^{-1}$. The use of heat flow calorimetry in larger scale (1.3 L), presented in this paper, resulted to be efficient and reproducible. The development of supercritical calorimetry required a very sensitive apparatus and good analysis of the heat transfer parameters.

## Conclusions

The newly developed supercritical reaction calorimeter allows measuring thermodynamical data such as reaction enthalpy and overall heat transfer coefficient used for process safety and optimization studies. The Wilson plot analysis allows understanding the heat transfer in supercritical carbon dioxide. It has been shown that the behavior of internal heat transfer coefficient in SCF is opposite of the one observed in classical liquids. The fundamental explanations are based on the particular tendency of the physicochemical properties of carbon dioxide to vary on a wide range close to its critical point. Moreover, it has been shown that the Nusselt correlation can also be used for heat transfer analysis in supercritical carbon dioxide.

Furthermore, it has been demonstrated that the polydimethylsiloxane macromonomer is a suitable stabilizer for the dispersion polymerization of methyl methacrylate under efficient stirring.

*Acknowledgement:* The *Swiss Commission for Technology and Innovation* n° 5254.1 and *Mettler-Toledo GmbH* are gratefully acknowledged for their support.

[1] A. Akergman, *ACS Symp. Ser.* **1997**, *670*, 208.
[2] P. G. Leitner, W. Jessop, "*Chemical synthesis using supercritical fluids*", Wiley-VCH, Weinheim 1999.
[3] W. Regenass, *J. Therm. Anal.* **1997**, *49*, 1661.
[4] H. F. Ferguson, D. J. Frurip, A. J. Pastor, L. M. Peery, L. F. Whiting, *Thermochim. Acta* **2000**, *363*, 1.
[5] F. Lavanchy, S. Fortini, Th. Meyer, *Chimia* **2002**, *56*, 126.
[6] D. A. Canelas, J. M. DeSimone, *Adv. Polym. Sci.* **1997**, *133*, 103.
[7] A. I. Cooper, *J. Mater. Chem.* **2000**, *10*, 207.
[8] A. J. Hyatt, *J. Org. Chem.* **1984**, *49*, 5097.
[9] A. I. Cooper, J. M. DeSimone, *Cur. Opin. Solid State Mater. Sci.* **1996**, *1*, 761.
[10] F. Rindfleisch, T. P. DiNoia, M. A. McHugh, *J. Phys. Chem.* **1996**, *100*, 15581.
[11] J. M. DeSimone, Z. Guanz, C. S. Elsbernd, *Science* **1992**, *257*, 945.
[12] J. M. DeSimone, E. E. Maury, Y. Z. Menceloglu, J. B. McClain, T. J. Romack, J. R. Combes, *Science* **1994**, *265*, 356.
[13] P. Christian, M. R. Giles, S. M. Howdle, R. C. Major, J. N. Hay, *Polymer* **2000**, *41*, 1251.
[14] Y. L. Hsiao, E. E. Maury, J. M. DeSimone, S. Mawson, K. P. Johnston, *Macromolecules* **1995**, *28*, 8159.
[15] M. L. O'Neill, M. Z. Yates, K. P. Johnston, C. D. Smith, S. P. Wilkinson, *Macromolecules* **1998**, *31*, 2838.
[16] M. L. O'Neill, M. Z. Yates, K. P. Johnston, C. D. Smith, S. P. Wilkinson, *Macromolecules* **1998**, *31*, 2848.
[17] K. A. Shaffer, T. A. Jones, D. A. Canelas, J. M. DeSimone, S. P. Wilkinson, *Macromolecules* **1996**, *29*, 2704.
[18] M. R. Giles, J. N. Hay, S. M. Howdle, R. J. Winder, *Polymer* **2000**, *41*, 6715.
[19] D. A. Canelas, D. E. Betts, J. M. DeSimone, *Macromolecules* **1996**, *29*, 2818.
[20] S. Fortini, F. Lavanchy, Th. Meyer, *Macromol. Symp.* **2004**, *206*, 79.
[21] F. Lavanchy, S. Fortini, Th. Meyer, *Org. Proc. Res. Develop.* **2004**, *8*, 504.
[22] E. E. Wilson, *Am. Soc. Chem. Eng.* **1915**, *37*, 47.
[23] G. Brooks, G.-J. Su, *Chem. Eng. Prog.* **1959**, *55*, 54.
[24] C. Lepilleur, E. J. Beckman, *Macromolecules* **1997**, *30*, 745.
[25] "*Polymer Handbook*", 3rd edition, J. Brandrup, E. H. Immergut, Eds., John Wiley & Sons, New York 1989.
[26] W. Wang, R. M. T. Griffiths, M. R. Giles, P. Williams, S. M. Howdle, *Eur. Polym. J.* **2003**, *39*, 423.

 